Acta Mech 225, 1323–1333 (2014)
DOI 10.1007/s00707-013-1045-5

H. T. Chen · A. K. Soh · Y. Ni

Phase field modeling of flexoelectric effects in ferroelectric epitaxial thin films

Received: 30 May 2013 / Revised: 12 September 2013 / Published online: 9 January 2014

Abstract The flexoelectric effect which is defined as the coupling between strain gradient and polarization has long been neglected because it is insignificant in bulk ferroelectrics. However, at nanoscale, the strain gradient can be dramatically increased leading to giant flexoelectric effects. In the present study, the flexoelectric effects in epitaxial nano thin films of a 180° multi-domain structure, which are subjected to a compressive in-plane misfit strain, are investigated by the phase field method. Unlike the case of a single domain structure where the strain gradient is mainly attributed to the formation of dislocation which relaxes the misfit strain, in a multi-domain structure, it is attributed to many factors, such as surface and interface effects, misfit relaxation and domain wall structure. The results obtained show that relatively large flexoelectricity-induced electric fields are produced near the domain wall region. The induced field will not only influence the domain structure of the thin film, but also the hysteresis loops when it is under an applied electric field.

1 Introduction

The flexoelectric effect that couples the polarization and strain gradient has been predicted [1] and then theoretically described [2] more than fifty years ago. However, this effect has been overlooked for nearly four decades due to its small magnitude for which the flexoelectric coefficients were theoretically estimated to be in the order of e/a, where e and a are the electronic charge and the lattice parameter, respectively. Nevertheless, the extensive experimental [3–7] and theoretical [8–14] works carried out in the past decade, on materials at nanoscale, showed that the strain gradient could be five or six orders of magnitude larger than that in bulk materials. Therefore, the flexoelectric effect can be quite significant or even dominant in nano thin films. Enhancement of piezoelectricity by 500 % was predicted in a $BaTiO_3$ nanobeam when the thickness of the beam was at several nanometers scale [15], and a giant imprint effect was observed in $HoMnO_3$ epitaxial

Presented at the 2013 SES Prager Medal Symposium in honor of Professor George Weng.

H. T. Chen
Department of Mechanical Engineering, The University of Hong Kong,
Hong Kong, People's Republic of China

A. K. Soh (✉)
School of Engineering, Monash University Sunway Campus,
Selangor, Malaysia
E-mail: soh.ai.kah@monash.edu

Y. Ni
CAS Key Laboratory of Mechanical Behavior and Design of Materials,
University of Science and Technology of China, Hefei 230026, Anhui,
People's Republic China

thin films [16]. The flexoelectric effect not only enlarges the range of piezoelectric materials [10,11,17], but also offers a totally new route for switching polarization in ferroelectrics [18,19]. In most previous works [8,20], one-dimensional assumption was always adopted to focus on the flexoelectric effects coupling with vertical strain gradient arising from the formation of dislocation by which the misfit strains were relieved. This simple assumption is helpful in achieving a preliminary understanding on the influence of flexoelectric effects. However, when both elastic energy and electrostatic energy are taken into consideration, the formation of a multi-domain structure is likely to be more energy preferable in epitaxial thin films that renders the one-dimensional assumption invalid. A recent experimental work [21] demonstrated that a horizontal strain gradient instead of vertical strain gradient can also cause a giant flexoelectric effect in dislocation-free epitaxial thin films. In order to achieve a better understanding of the influence of the flexoelectric effect in epitaxial thin films, an attempt is made in the present study to perform a rough estimation of the said effect by considering not only the strain gradient arising from the misfit strain relaxation, but also that due to domain formation.

2 Phase field modeling

A phase field model is developed to investigate the flexoelectric effects in epitaxial thin films. Conventionally, the total free energy of the system can be expressed as:

$$F^0 = \iiint \left(f_{\text{bulk}} + f_{\text{grad}} + f_{\text{elec}} + f_{\text{elas}}\right) \mathrm{d}x_1 \mathrm{d}x_2 \mathrm{d}x_3 + \iint f_s \mathrm{d}x_1 \mathrm{d}x_2, \tag{1}$$

where f_{bulk}, f_{grad}, f_{elec}, f_{elas} and f_s are the bulk free energy density, domain wall energy density, electric energy density, elastic energy density and surface energy density, respectively.

The bulk free energy density can be described by the conventional Landau-type extension, which can be expressed as:

$$\begin{aligned} f_{\text{bulk}} = {} & \alpha_1 \left(P_1^2 + P_2^2 + P_3^2\right) + \alpha_{11} \left(P_1^4 + P_2^4 + P_3^4\right) + a_{12} \left(P_1^2 P_2^2 + P_2^2 P_3^2 + P_3^2 P_1^2\right) \\ & + \alpha_{111} \left(P_1^6 + P_2^6 + P_3^6\right) + \alpha_{112} \left[P_1^2 \left(P_2^2 + P_3^2\right) + P_1^2 \left(P_1^2 + P_3^2\right) + P_1^2 \left(P_1^2 + P_2^2\right)\right] \\ & + \alpha_{123} P_1^2 P_2^2 P_2^2, \end{aligned} \tag{2}$$

where $\alpha_1, \alpha_{11}, \alpha_{12}, \alpha_{111}, \alpha_{112}, \alpha_{123}$ are the phenomenological Landau expansion coefficients.

The domain wall energy density is given by:

$$\begin{aligned} f_{\text{grad}} = {} & \frac{1}{2} g_{11} \left(P_{1,1}^2 + P_{2,2}^2 + P_{3,3}^2\right) + g_{12} \left(P_{1,1} P_{2,2} + P_{2,2} P_{3,3} + P_{3,3} P_{1,1}\right) \\ & + \frac{1}{2} g_{44} \left[\left(P_{1,2} + P_{2,1}\right)^2 + \left(P_{2,3} + P_{3,2}\right)^2 + \left(P_{1,3} + P_{3,1}\right)^2\right] \\ & + \frac{1}{2} g'_{44} \left[\left(P_{1,2} - P_{2,1}\right)^2 + \left(P_{2,3} - P_{3,2}\right)^2 + \left(P_{1,3} - P_{3,1}\right)^2\right], \end{aligned} \tag{3}$$

where g_{11}, g_{44} and g'_{44} are the gradient coefficients, and the commas in the subscripts denote spatial differentiation.

The electric energy can be presented as [22]:

$$\iiint f_{\text{elec}} \mathrm{d}x_1 \mathrm{d}x_2 \mathrm{d}x_3 = \frac{1}{2\varepsilon} \iiint_{|\xi| \neq 0} \frac{d^3 \xi}{(2\pi)^3} |\mathbf{P}(\boldsymbol{\xi}) \cdot \mathbf{k}|^2 - \iiint E_i^{ex} P_i \mathrm{d}x_1 \mathrm{d}x_2 \mathrm{d}x_3, \tag{4}$$

where $\mathbf{P}(\boldsymbol{\xi}) = \int \frac{d^3 \mathbf{x}}{(2\pi)^3} \mathbf{P}(\mathbf{x}) e^{-i \boldsymbol{\xi} \cdot \mathbf{x}}$ is the Fourier transformation of the polarization field $\mathbf{P}(\mathbf{r})$, $\mathbf{k} = (k_1, k_2, k_3) = (\xi_1, \xi_2, \xi_3)/|\boldsymbol{\xi}|$ is the unit vector in the reciprocal Fourier space, and $\varepsilon = \varepsilon_r \varepsilon_0$ is the dielectric constant of ferroelectric material with $\varepsilon_0 = 8.85 \times 10^{12}\,\text{Fm}^{-1}$ the dielectric constant in the vacuum, and ε_r the relative dielectric constant.

The elastic energy density can be expressed as:

$$f_{\text{elas}} = \frac{1}{2} c_{ijkl} e_{ij} e_{kl} = \frac{1}{2} \sigma_{ij} \left(\varepsilon_{ij} - \varepsilon_{ij}^*\right), \tag{5}$$

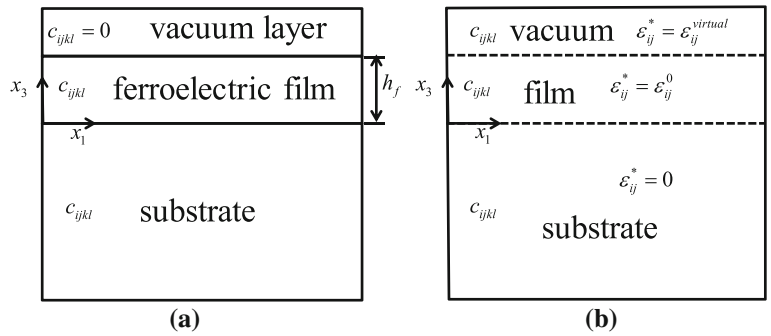

Fig. 1 **a** Schematic of a film–substrate simulation system, where h_f denotes the thickness of the ferroelectric film; **b** the equivalent elastically homogeneous system with c_{ijkl} and the properly distributed stress-free strain ε_{ij}^{*}

where c_{ijkl}, σ_{ij}, e_{ij}, ε_{ij} and ε_{ij}^{*} are the elastic stiffness, elastic stress, elastic strain, total strain and stress-free strain, respectively. As shown in Fig. 1, calculating the elastic strain in the original heterogeneous film–substrate system (Fig. 1a) can be replaced by calculating the elastic strain in the equivalent elastically homogeneous system with constant c_{ijkl} and the properly distributed stress-free strain (Fig. 1b) by using a phase field microelasticity model [23,24]. The stress-free strain is zero in the substrate, is equal to the electrostrictive-related strain ε_{ij}^{0} in the ferroelectric film, and is equal to the virtual strain $\varepsilon_{ij}^{virtual}$ in the vacuum layer. The electrostrictive strains are dependent on electric polarization which can be expressed as:

$$\begin{aligned}
\varepsilon_{11}^{0} &= Q_{11}P_1^2 + Q_{12}\left(P_2^2+P_3^2\right), \varepsilon_{12}^{0} = Q_{44}P_1P_2,\\
\varepsilon_{22}^{0} &= Q_{11}P_2^2 + Q_{12}\left(P_1^2+P_3^2\right), \varepsilon_{23}^{0} = Q_{44}P_2P_3,\\
\varepsilon_{33}^{0} &= Q_{11}P_3^2 + Q_{12}\left(P_1^2+P_3^2\right), \varepsilon_{13}^{0} = Q_{44}P_1P_3,
\end{aligned} \tag{6}$$

where Q_{11}, Q_{12} and Q_{44} are the electrostrictive coefficients. The virtual strains $\varepsilon_{ij}^{virtual}$ are introduced to satisfy the free surface boundary conditions [23,24].

The surface energy density is given by:

$$f_s = a_{11}^{S}\left(P_1^2+P_2^2+P_3^2\right), \tag{7}$$

where a_{11}^{S} is the surface Landau expansion coefficient.

When flexoelectric effects in the system are taken into consideration, the additional energy term F_{flex} related to flexoelectricity, which should be incorporated in the total free energy, can be expressed as [12,13]:

$$F_{\text{flex}} = -\iiint \frac{f_{ijkl}}{2}\left(P_k\frac{\partial\varepsilon_{ij}}{\partial x_l} - \varepsilon_{ij}\frac{\partial P_k}{\partial x_l}\right)\mathrm{d}x_1\mathrm{d}x_2\mathrm{d}x_3, \quad (i,j,k,l=1,2,3), \tag{8}$$

where f_{ijkl} are the flexoelectric coefficients. Hence, the total free energy can be expressed as $F = F^0 + F_{\text{flex}}$. The variation of the total free energy with polarizations and strains yield Euler-Lagrange equations incorporated with the boundary conditions [25–27] as follows:

$$\left(a_{ij}^{S}P_j + g_{ijkl}\frac{\partial P_k}{\partial x_l}n_j + \frac{f_{ijkl}}{2}\varepsilon_{kl}n_j\right)|_S = 0, \tag{9.1}$$

$$\left(\sigma_{ij}n_j + \theta_{ijk,l}n_jn_kn_l - \theta_{ijk,j}n_k\right)|_S = 0, \tag{9.2}$$

where $\theta_{ijk} = -1/2\, f_{ijkl}P_l$, and $\mathbf{n}$ is the outward normal unit vector of the surface. The flexoelectricity-induced electric field arising from the variation of the free energy with polarization is given by:

$$E_i^{\text{flex}} = -\frac{\delta F_{\text{flex}}}{\delta P_i} = f_{ijkl}\frac{\partial\varepsilon_{kl}}{\partial x_j}. \tag{10}$$

Moreover, the flexoelectricity-induced stress field can be obtained based on the variation of the free energy with total strain:

$$\sigma_{ij}^{\text{flex}} = \frac{\delta F_{\text{flex}}}{\delta\varepsilon_{ij}} = f_{ijkl}\frac{\partial P_k}{\partial x_l}. \tag{11}$$

By employing the Voigt notation that $f_{1111} = f_{11}, f_{1122} = f_{12}, f_{1212} = f_{44}, c_{1111} = c_{11}, c_{1122} = c_{12}, c_{1212} = c_{44}$, the flexoelectricity-induced electric field can be expressed as:

$$E_1^{\text{flex}} = f_{11}\frac{\partial \varepsilon_{11}}{\partial x_1} + 2f_{44}\left(\frac{\partial \varepsilon_{12}}{\partial x_2} + \frac{\partial \varepsilon_{13}}{\partial x_3}\right) + f_{12}\left(\frac{\partial \varepsilon_{22}}{\partial x_1} + \frac{\partial \varepsilon_{33}}{\partial x_1}\right), \tag{12.1}$$

$$E_2^{\text{flex}} = f_{11}\frac{\partial \varepsilon_{22}}{\partial x_1} + 2f_{44}\left(\frac{\partial \varepsilon_{12}}{\partial x_1} + \frac{\partial \varepsilon_{23}}{\partial x_3}\right) + f_{12}\left(\frac{\partial \varepsilon_{11}}{\partial x_2} + \frac{\partial \varepsilon_{33}}{\partial x_2}\right), \tag{12.2}$$

$$E_3^{\text{flex}} = f_{11}\frac{\partial \varepsilon_{33}}{\partial x_1} + 2f_{44}\left(\frac{\partial \varepsilon_{23}}{\partial x_2} + \frac{\partial \varepsilon_{31}}{\partial x_1}\right) + f_{12}\left(\frac{\partial \varepsilon_{11}}{\partial x_3} + \frac{\partial \varepsilon_{22}}{\partial x_3}\right). \tag{12.3}$$

Similarly, the flexoelectricity-related stress can be expressed as:

$$\sigma_{11}^{\text{flex}} = f_{11}\frac{\partial P_1}{\partial x_1} + f_{12}\left(\frac{\partial P_2}{\partial x_2} + \frac{\partial P_3}{\partial x_3}\right), \tag{13.1}$$

$$\sigma_{22}^{\text{flex}} = f_{11}\frac{\partial P_2}{\partial x_2} + f_{12}\left(\frac{\partial P_1}{\partial x_1} + \frac{\partial P_3}{\partial x_3}\right), \tag{13.2}$$

$$\sigma_{33}^{\text{flex}} = f_{11}\frac{\partial P_3}{\partial x_3} + f_{12}\left(\frac{\partial P_1}{\partial x_1} + \frac{\partial P_2}{\partial x_2}\right), \tag{13.3}$$

$$\sigma_{12}^{\text{flex}} = \sigma_{21}^{\text{flex}} = f_{44}\left(\frac{\partial P_1}{\partial x_2} + \frac{\partial P_2}{\partial x_1}\right), \tag{13.4}$$

$$\sigma_{13}^{\text{flex}} = \sigma_{31}^{\text{flex}} = f_{44}\left(\frac{\partial P_1}{\partial x_3} + \frac{\partial P_3}{\partial x_1}\right), \tag{13.5}$$

$$\sigma_{23}^{\text{flex}} = \sigma_{32}^{\text{flex}} = f_{44}\left(\frac{\partial P_2}{\partial x_3} + \frac{\partial P_3}{\partial x_2}\right). \tag{13.6}$$

The boundary conditions given by Eq. (9.1) can be rewritten as:

$$\begin{aligned}
&a_1^S P_1 - \left(g_{44} - \frac{2f_{44}^2}{c_{44}}\right)\frac{\partial P_1}{\partial x_3} = 0,\\
&a_1^S P_2 - \left(g_{44} - \frac{2f_{44}^2}{c_{44}}\right)\frac{\partial P_2}{\partial x_3} = 0 \quad (x_3 = 0),\\
&a_1^S P_3 - \left(g_{11} - \frac{f_{11}^2}{2c_{11}}\right)\frac{\partial P_3}{\partial x_3} = 0,
\end{aligned} \tag{14.1}$$

$$\begin{aligned}
&a_1^S P_1 + \left(g_{44} - \frac{2f_{44}^2}{c_{44}}\right)\frac{\partial P_1}{\partial x_3} = 0,\\
&a_1^S P_2 + \left(g_{44} - \frac{2f_{44}^2}{c_{44}}\right)\frac{\partial P_2}{\partial x_3} = 0 \quad (x_3 = h_f),\\
&a_1^S P_3 + \left(g_{11} - \frac{f_{11}^2}{2c_{11}}\right)\frac{\partial P_3}{\partial x_3} = 0,
\end{aligned} \tag{14.2}$$

The detailed deduction of the boundary conditions is presented in the "Appendix".

The dynamic evolution of virtual stress-free strains and polarization are governed by the time dependent Ginzburg-Landau (TDGL) equations [23,28]:

$$\frac{\partial \varepsilon_{ij}^{virtual}(\mathbf{x}, t)}{\partial t} = -K\frac{\delta F}{\delta \varepsilon_{ij}^{virtual}(\mathbf{x}, t)}, \tag{15}$$

$$\frac{\partial P_i(\mathbf{x}, t)}{\partial t} = -L\frac{\delta F}{\delta P_i(\mathbf{x}, t)}, \tag{16}$$

where K and L are kinetic coefficients.

3 Simulation parameters and methodology

A two-dimensional simulation system consisting of $192\Delta x_1 \times 58\Delta x_3$ discrete grids with grid size $\Delta x_1 = \Delta x_3 = dl = 1nm$ in real space is devised for the present study. The system encompasses three parts, i.e., a top part of 8 layers, a bottom part of 20 layers and a middle portion representing the vacuum region, the substrate and the $BaTiO_3$ ferroelectric thin film, respectively. Therefore, the thickness of the film is 30nm. The periodic boundary conditions are applied along the x_1 and x_3 direction. For simplicity, the film–substrate system is assumed to be elastically homogeneous. The coefficients used in the simulation are listed below [7,24,29,30]:

$$\begin{aligned}
&\alpha_1 = 3.3(T-110)\times 10^5\,\mathrm{C^{-2}m^2\,N}, \quad \alpha_{11} = 3.6(T-115)\times 10^6\mathrm{C^{-4}\,m^6\,N},\\
&\alpha_{12} = 4.9\times 10^8\mathrm{C^{-4}\,m^6\,N}, \quad \alpha_{111} = 6.6\times 10^9\mathrm{C^{-6}\,m^{10}\,N}, \quad \alpha_{112} = 2.9\times 10^9\mathrm{C^{-6}\,m^{10}\,N},\\
&Q_{11} = 0.11\mathrm{C^{-2}\,m^4}, \quad Q_{12} = -0.043\mathrm{C^{-2}\,m^4}, \quad Q_{44} = 0.059\mathrm{C^{-2}\,m^4},\\
&c_{11} = 1.78\times 10^{11}\,\mathrm{Nm^{-2}}, \quad c_{12} = 0.96\times 10^{11}\,\mathrm{Nm^{-2}}, \quad c_{44} = 1.22\times 10^{11}\,\mathrm{Nm^{-2}},\\
&f_{11} = 0.2\times 10^{-9}\,\mathrm{Cm^{-1}}/\varepsilon, \quad f_{12} = 7.0\times 10^{-9}\,\mathrm{Cm^{-1}}/\varepsilon, \quad f_{44} = 3.0\times 10^{-9}\,\mathrm{Cm^{-1}}/\varepsilon, \quad \varepsilon_r = 1{,}100.
\end{aligned}$$

Due to a lack of experimental data for the complete set of flexoelectric coefficients for $BaTiO_3$, in the present study, the coefficients of $SrTiO_3$ are adopted, which are expected to produce qualitatively valid results. The reference value of the gradient energy coefficient is g_{110} and $dl = \sqrt{g_{110}/|\alpha_0|}$. The values of gradient coefficients $g_{11}/g_{110} = 3.2$ and $g_{44}/g_{110} = g'_{44}/g_{110} = 1.6$ are adopted. The simulation temperature is as assumed to be 25 °C. The spontaneous polarization is $P_0 = 0.26\,\mathrm{Cm^{-2}}$, and the extrapolation lengths are $\lambda_1 = g_{11}/a_1^S = 1\,\mathrm{nm}$ and $\lambda_3 = g_{44}/a_1^S = 0.5\,\mathrm{nm}$. Thus, the boundary conditions given in Eq. (14) can be expressed in terms of the extrapolation lengths as follows:

$$\frac{\partial P_i}{\partial x_3}|_{x_3=0} = P_i/\lambda_i, \quad \frac{\partial P_i}{\partial x_3}|_{x_3=h_f} = -P_i/\lambda_i, \quad (i=1,3). \tag{17}$$

Note that a positive extrapolation length implies that the polarization in the boundary layer has a smaller value compared with that in the middle layers. In the simulation system with discrete grids along the x_3 axis, the polarization of the boundary layers can be calculated by [31,32]:

$$P_{i,x_3=0} = \frac{4P_{i,x_3=1} - P_{i,x_3=2}}{3+2\Delta x_3/\lambda_i} \quad \text{and} \quad P_{i,x_3=h_f} = \frac{4P_{i,x_3=h_f-1} + P_{i,x_3=h_f-2}}{3+2\Delta x_3/\lambda_i}. \tag{18}$$

In most theoretical works, the misfit strains in the film–substrate system are assumed as constant values based on the lattice mismatch between the film and substrate. However, there is both theoretical [8,33] and experimental [16,34] evidence that the misfit strains relax with thickness. Thus, an exponential relaxation is usually adopted to describe the misfit strain as follow:

$$\varepsilon_{11}^{misfit} = \varepsilon_0^{misfit} e^{-x_3/\delta}, \tag{19}$$

where ε_0^{misfit} is the lattice mismatch between the film and substrate, and δ is the thickness at which the strain has relaxed to $1/e$ of the said mismatch. The value of δ is varied from hundreds to tens of nanometers. In the present study, the values of 100nm and -0.005 are adopted for δ and ε_0^{misfit}, respectively. In the phase field model, the total strain is composed of both homogenous and heterogeneous strain. The former describes the macroscopic deformation of the system. For the epitaxial thin film, the homogenous strain is mainly determined by the misfit strain. Therefore, in the present study, the homogenous strain of the film is deemed equal to the misfit strain, i.e., $\bar{\varepsilon}_{11} = \varepsilon_{11}^{misfit}$, and $\bar{\varepsilon}_{13}$ & $\bar{\varepsilon}_{33}$ can be obtained from the equation $c_{i3kl}\bar{\varepsilon}_{kl} = 0$. Note that the $\bar{\varepsilon}_{i3}$ determined here are only part of the total shape deformation of the film [32,35].

4 Results and discussion

Figure 2 shows the domain structure of a $BaTiO_3$ ferroelectric thin film without considering the flexoelectric effects. The polarization is aligned either upward or downward, forming a typical 180° multi-domain structure. In order to reduce the elastic and electrostatic energy, multi-domain structures rather than single domain structures are more likely to form in epitaxial thin films. However, for simplicity, most of the existing

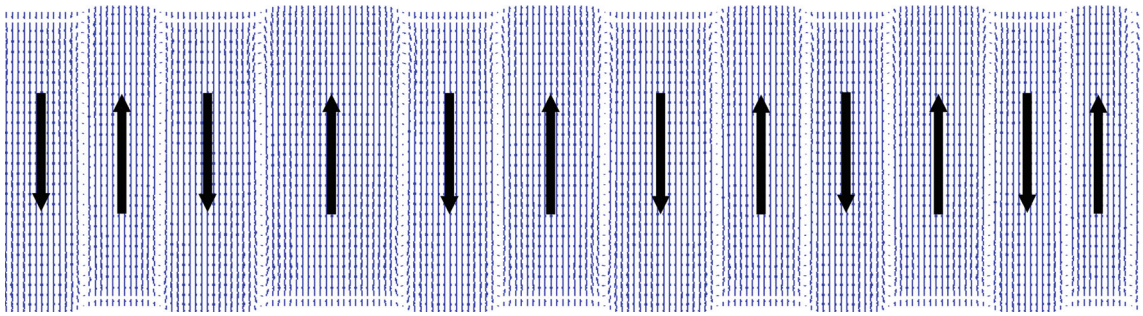

Fig. 2 Multi-domain structure: a $BaTiO_3$ ferroelectric thin film with flexoelectric effect neglected (The *arrows* denote the polarization direction)

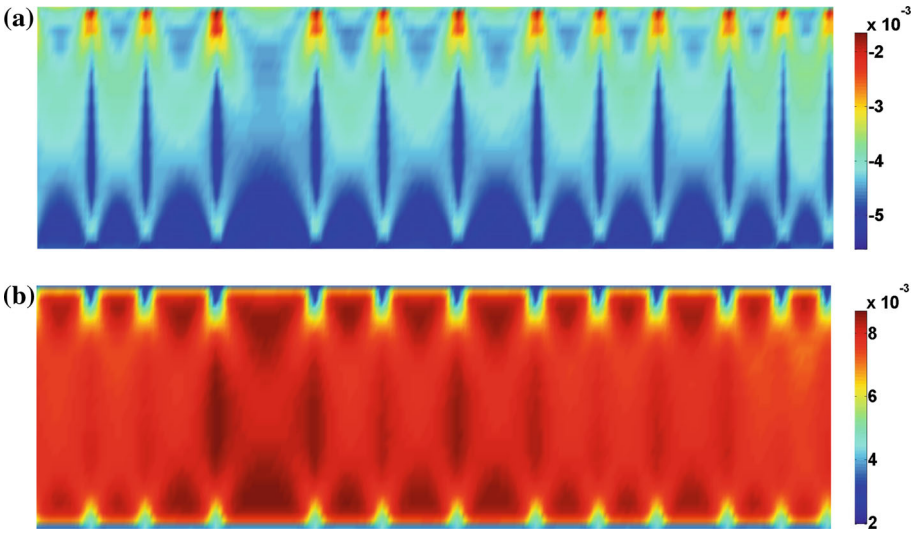

Fig. 3 Contour plots of the total **a** in-plane strain ε_{11} and **b** out-of-plane strain ε_{33} in a thin film

theoretical works on flexoelectric effects in nano thin films were carried out based on the assumption of a single domain structure. Thus, there is a necessity to study the flexoelectric effects in the more realistic situation of a multi-domain structure. Figure 3a, b presents the contour plots of the in-plane and out-of-plane total strains, respectively. Although a rough trend of in-plane strain relaxation along the thickness can be observed, the strain gradient is more visible in the region near the domain wall. Moreover, due to the interfacial and surface effects, the film shows a strong inhomogeneous strain state near the interfacial and surface regions. These results clearly demonstrate that the strain gradient in a multi-domain epitaxial thin film is no longer dominated by the strain relaxation along the thickness as that in the case of single domain film. The large strain gradient near the domain wall is expected to produce a large flexoelectricity-induced electric field that could have significant influence on the domain structure, especially in a film with high domain wall density.

Figure 4a, b present the flexoelectricity-induced in-plane and out-of-plane electric fields, respectively, in a $BaTiO_3$ ferroelectric thin film. Note that the electric fields described here and hereafter are normalized as $E/|\alpha_0 P_0|$. Due to the small magnitude of the induced fields, the domain structure shows little change. Although the in-plane field E_1^{flex} is nearly zero in most regions of the thin film, it possesses relatively large values in the domain wall region near the free surface and film–substrate interface. Similarly, relatively large values of the out-of-plane field E_3^{flex} can be observed in the domain wall region near the free surface and film–substrate interface. However, E_3^{flex} has small positive values in the middle of the film. In order to achieve a better understanding of the flexoelectric effect, a detailed investigation of the formula for the flexoelectric field given by Eq. (12.1), i.e., $E_1^{\text{flex}} = f_{11}\frac{\partial \varepsilon_{11}}{\partial x_1} + 2f_{44}\frac{\partial \varepsilon_{13}}{\partial x_3} + f_{12}\frac{\partial \varepsilon_{33}}{\partial x_1}$, is carried out. The longitudinal flexoelectric coefficient f_{11} is one order of magnitude smaller than the transverse flexoelectric coefficient f_{12}. Although the

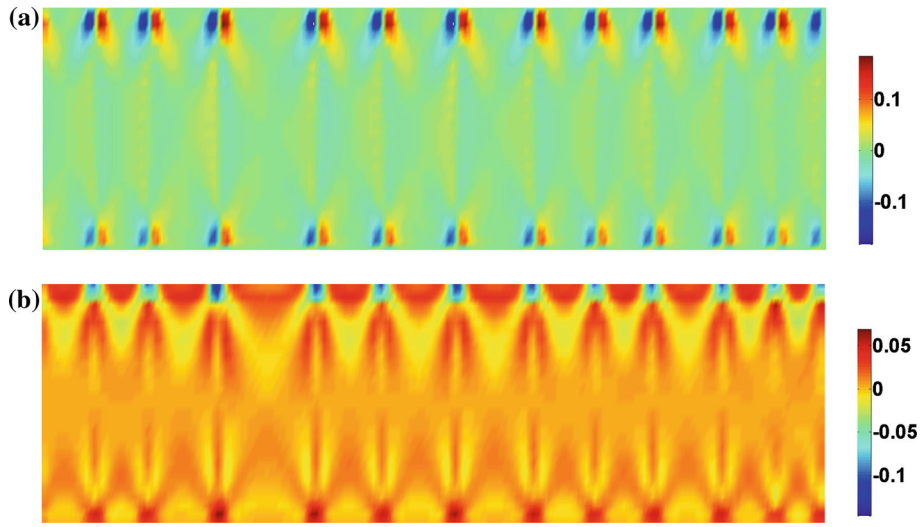

Fig. 4 Flexoelectricity-induced electric field **a** E_1^{flex} and **b** E_3^{flex} in a thin film

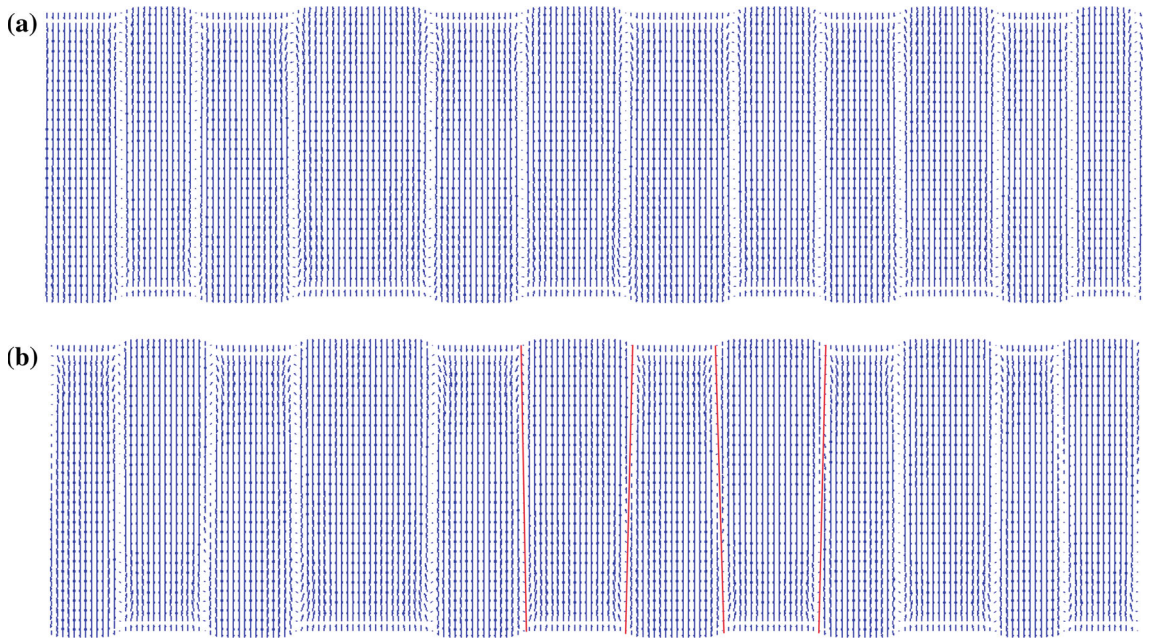

Fig. 5 Domain structures arising from different flexoelectric coefficients **a** f_{ij} and **b** $5f_{ij}$ (*the red solid lines* denote the domain walls)

shear flexoelectric coefficient f_{44} is comparable with the transverse one, the calculated shear strain is one order of magnitude smaller than the normal strains. Therefore, out of the three attributions which are counted for, only the last term $f_{12}\frac{\partial \varepsilon_{33}}{\partial x_1}$ has an important influence on the field E_1^{flex}. A similar conclusion can be drawn on E_3^{flex}, i.e., the term $f_{12}\frac{\partial \varepsilon_{33}}{\partial x_3}$ plays the most important role. Obviously, the misfit strain makes no contributions to E_1^{flex}, but it produces a positive field to E_3^{flex}, which is consistent with the distribution of the flexoelectric field, as shown in Fig. 4.

Figure 5 compares the domain structures arising from two different sets of flexoelectric coefficients. The second set of coefficients is selected as five times that of the first set to clearly show the influence of the flexoelectric effect. Thus, an obvious evolution of domain structure can be observed in Fig. 5. First, the domain regions with positive out-of-plane polarization (c^+ domain) are enlarged, while those with negative out-of-plane polarization (c^- domain) are shrunk. Consequently, the ratio of c^+/c^- is changed from

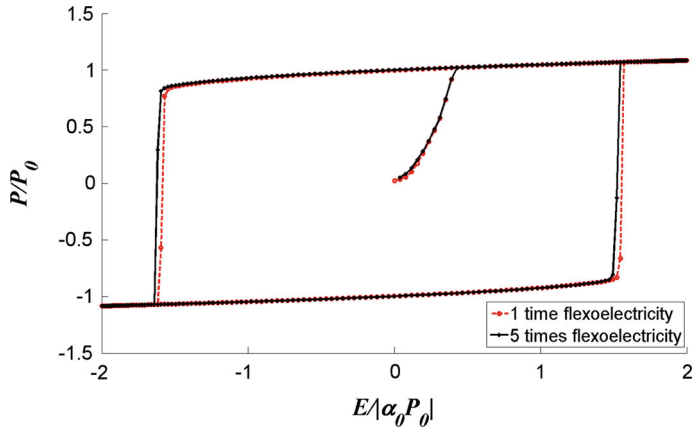

Fig. 6 P–E hysteresis loops with different values of flexoelectric coefficients

1.04:1 to 1.24:1. This change is attributed to the positive flexoelectric field along the thickness direction arising from the in-plane misfit strain gradient. Moreover, by observing the domain structure carefully, one would find that the enlargement of c^+ domains is not homogeneous along the thickness direction. In fact, the region near the free surface is more enlarged compared with that near the film–substrate interface, as depicted in Fig. 5b. With the increase in the flexoelectricity-induced electric field, it is reasonable to predict that the domain structure with a stripe pattern would be replaced by a serration domain pattern. The formation of a serration domain pattern has been demonstrated in a recent experiment, in which a giant flexoelectricity-induced electric field was produced by manipulating the misfit strain relaxation length [16].

Figure 6 presents the P-E hysteresis loops plotted for a ferroelectric thin film with different values of flexoelectric coefficients subjected to an applied electric field along the thickness direction. A shift of the hysteresis loop along the negative abscissa axis indicates a positive built-in field. Thus, the formula $E_{\text{in}} = -(E_{\text{c}}^{+} + E_{\text{c}}^{-})/2$, where E_{in}, E_{c}^{+} and E_{c}^{-} denote the built-in field and the positive and negative coercive field, respectively, is used to calculate the flexoelectricity-induced built-in field. The calculated built-in fields for a thin film with one and five times the original flexoelectric coefficients selected for simulation are 0.014 and 0.050, respectively, which are small compared with the coercive field, but by no means insignificant.

5 Conclusions

A two-dimensional phase field model is devised to study the flexoelectric effects in epitaxial thin films. A detailed illustration on the existence of flexoelectricity-induced electric fields is presented based on the precision solution of strain states. Both in-plane and out-of plane electric fields are observed, and their values are relatively large in the domain wall region near the free surface and film–substrate interface. This result is quite different from that obtained in the case of a single domain structure, in which only the out-of-plane electric field is produced due to the misfit strain relaxation along the thickness direction. When the thin ferroelectric film is subjected to an external electric field, a built-in field arising from the flexoelectric effect can be observed in the hysteresis loops. It is worth noting that in an epitaxial thin film there are many factors that could influence the strain gradient, such as the film thickness, the magnitude of lattice mismatch between film–substrate and the relaxation length of the mismatch strain. Further studies will be carried out in future to investigate the influence of these factors.

Acknowledgments This work was supported by Research Grants Council of the Hong Kong Special Administrative Region (Project no. HKU 717011E) and Monash University Sunway Campus Research Grant. Yong Ni gratefully appreciates financial supports from the Chinese Natural Science Foundation (Grant No. 11222219).

Appendix

The boundary conditions in Eq. (9.1) can be expressed as:

$$
\begin{aligned}
&a_1^S P_1 - g_{44}\left(\frac{\partial P_1}{\partial x_3} + \frac{\partial P_3}{\partial x_1}\right) - f_{44}\varepsilon_{13} = 0,\\
&a_1^S P_2 - g_{44}\left(\frac{\partial P_2}{\partial x_3} + \frac{\partial P_3}{\partial x_2}\right) - f_{44}\varepsilon_{23} = 0 \qquad (x_3 = 0),\\
&a_1^S P_3 - g_{11}\frac{\partial P_3}{\partial x_3} - g_{12}\left(\frac{\partial P_1}{\partial x_1} + \frac{\partial P_2}{\partial x_2}\right) - \frac{f_{12}}{2}(\varepsilon_{11} + \varepsilon_{22}) - \frac{f_{11}}{2}\varepsilon_{33} = 0,
\end{aligned}
\tag{A1.1}
$$

$$
\begin{aligned}
&a_1^S P_1 + g_{44}\left(\frac{\partial P_1}{\partial x_3} + \frac{\partial P_3}{\partial x_1}\right) + f_{44}\varepsilon_{13} = 0,\\
&a_1^S P_2 + g_{44}\left(\frac{\partial P_2}{\partial x_3} + \frac{\partial P_3}{\partial x_2}\right) + f_{44}\varepsilon_{23} = 0 \qquad (x_3 = h_f),\\
&a_1^S P_3 + g_{11}\frac{\partial P_3}{\partial x_3} + g_{12}\left(\frac{\partial P_1}{\partial x_1} + \frac{\partial P_2}{\partial x_2}\right) + \frac{f_{12}}{2}(\varepsilon_{11} + \varepsilon_{22}) + \frac{f_{11}}{2}\varepsilon_{33} = 0.
\end{aligned}
\tag{A1.2}
$$

And the boundary conditions in Eq. (9.2) can be written as:

$$
\begin{aligned}
&\sigma_{13} - \frac{f_{12}}{2}\frac{\partial P_3}{\partial x_1} = 0,\\
&\sigma_{23} - \frac{f_{12}}{2}\frac{\partial P_3}{\partial x_2} = 0 \qquad (x_3 = 0),\\
&\sigma_{33} - \frac{f_{44}}{2}\left(\frac{\partial P_1}{\partial x_1} + \frac{\partial P_2}{\partial x_2}\right) = 0,
\end{aligned}
\tag{A2.1}
$$

$$
\begin{aligned}
&\sigma_{13} + \frac{f_{12}}{2}\frac{\partial P_3}{\partial x_1} = 0,\\
&\sigma_{23} + \frac{f_{12}}{2}\frac{\partial P_3}{\partial x_2} = 0 \qquad (x_3 = h_f),\\
&\sigma_{33} + \frac{f_{44}}{2}\left(\frac{\partial P_1}{\partial x_1} + \frac{\partial P_2}{\partial x_2}\right) = 0.
\end{aligned}
\tag{A2.2}
$$

From the stress expression:

$$
f_{ijkl}\frac{\partial P_k}{\partial x_l} + c_{ijkl}\left(\varepsilon_{kl} - \varepsilon_{kl}^0\right) = \sigma_{ij} \tag{A.3}
$$

we obtain at $x_3 = 0$

$$
\begin{aligned}
\varepsilon_{13} &= \frac{1}{c_{44}}\left(2\sigma_{13} - 2f_{44}\frac{\partial P_1}{\partial x_3} - 2f_{44}\frac{\partial P_3}{\partial x_1}\right) + \varepsilon_{13}^0 = \frac{1}{c_{44}}\left(f_{12}\frac{\partial P_3}{\partial x_1} - 2f_{44}\frac{\partial P_1}{\partial x_3} - 2f_{44}\frac{\partial P_3}{\partial x_1}\right) + \varepsilon_{13}^0,\\
\varepsilon_{23} &= \frac{1}{c_{44}}\left(2\sigma_{23} - 2f_{44}\frac{\partial P_2}{\partial x_3} - 2f_{44}\frac{\partial P_3}{\partial x_2}\right) + \varepsilon_{23}^0 = \frac{1}{c_{44}}\left(f_{12}\frac{\partial P_3}{\partial x_2} - 2f_{44}\frac{\partial P_1}{\partial x_3} - 2f_{44}\frac{\partial P_3}{\partial x_2}\right) + \varepsilon_{23}^0,\\
\varepsilon_{33} &= \frac{1}{c_{12}}\left[\sigma_{11} + \sigma_{22} - (f_{11}+f_{12})\left(\frac{\partial P_1}{\partial x_1} + \frac{\partial P_2}{\partial x_2}\right) - 2f_{12}\frac{\partial P_3}{\partial x_3}\right] + \frac{1}{c_{11}}\left[\sigma_{33} - f_{12}\left(\frac{\partial P_1}{\partial x_1} + \frac{\partial P_2}{\partial x_2}\right) - f_{11}\frac{\partial P_3}{\partial x_3}\right] + \varepsilon_{33}^0;
\end{aligned}
\tag{A4.1}
$$

at $x_3 = h_f$

$$
\begin{aligned}
\varepsilon_{13} &= \frac{1}{c_{44}}\left(2\sigma_{13} - 2f_{44}\frac{\partial P_1}{\partial x_3} - 2f_{44}\frac{\partial P_3}{\partial x_1}\right) + \varepsilon_{13}^0 = \frac{1}{c_{44}}\left(-f_{12}\frac{\partial P_3}{\partial x_1} - 2f_{44}\frac{\partial P_1}{\partial x_3} - 2f_{44}\frac{\partial P_3}{\partial x_1}\right) + \varepsilon_{13}^0,\\
\varepsilon_{23} &= \frac{1}{c_{44}}\left(2\sigma_{23} - 2f_{44}\frac{\partial P_2}{\partial x_3} - 2f_{44}\frac{\partial P_3}{\partial x_2}\right) + \varepsilon_{23}^0 = \frac{1}{c_{44}}\left(-f_{12}\frac{\partial P_3}{\partial x_2} - 2f_{44}\frac{\partial P_1}{\partial x_3} - 2f_{44}\frac{\partial P_3}{\partial x_2}\right) + \varepsilon_{23}^0,\\
\varepsilon_{33} &= \frac{1}{c_{12}}\left[\sigma_{11} + \sigma_{22} - (f_{11}+f_{12})\left(\frac{\partial P_1}{\partial x_1} + \frac{\partial P_2}{\partial x_2}\right) - 2f_{12}\frac{\partial P_3}{\partial x_3}\right] + \frac{1}{c_{11}}\left[\sigma_{33} - f_{12}\left(\frac{\partial P_1}{\partial x_1} + \frac{\partial P_2}{\partial x_2}\right) - f_{11}\frac{\partial P_3}{\partial x_3}\right] + \varepsilon_{33}^0.
\end{aligned}
\tag{A4.2}
$$

By substituting the expressions for strains ε_{i3} in Eq. (A4) into Eq. (A1), the boundary conditions can be rewritten as:

$$\begin{aligned}
&a_1^S P_1 - \left(g_{44} - \frac{2f_{44}^2}{c_{44}}\right)\frac{\partial P_1}{\partial x_3} - \left[g_{44} + \frac{f_{44}\left(f_{12} - 2f_{44}\right)}{c_{44}}\right]\frac{\partial P_3}{\partial x_1} - f_{44}\varepsilon_{13}^0 = 0\\
&a_1^S P_2 - \left(g_{44} - \frac{2f_{44}^2}{c_{44}}\right)\frac{\partial P_2}{\partial x_3} - \left[g_{44} + \frac{f_{44}\left(f_{12} - 2f_{44}\right)}{c_{44}}\right]\frac{\partial P_3}{\partial x_2} - f_{44}\varepsilon_{23}^0 = 0\\
&a_1^S P_3 - \left[g_{12} - \frac{f_{11}\left(f_{12} - \frac{1}{2}f_{44}\right)}{2c_{44}}\right]\left(\frac{\partial P_1}{\partial x_1} + \frac{\partial P_2}{\partial x_2}\right) - \left(g_{11} - \frac{f_{11}^2}{2c_{11}}\right)\frac{\partial P_3}{\partial x_3}\\
&\quad - \frac{1}{2}\left(f_{12} - \frac{c_{12}}{c_{11}}f_{11}\right)\left(\varepsilon_{11} + \varepsilon_{22}\right) - \frac{1}{2}f_{11}\left(\frac{c_{12}}{c_{11}}\varepsilon_{11}^0 + \frac{c_{12}}{c_{11}}\varepsilon_{22}^0 + \varepsilon_{33}^0\right) = 0;
\end{aligned} \qquad (x_3 = 0), \qquad \text{(A5.1)}$$

$$\begin{aligned}
&a_1^S P_1 + \left(g_{44} - \frac{2f_{44}^2}{c_{44}}\right)\frac{\partial P_1}{\partial x_3} + \left[g_{44} + \frac{f_{44}\left(-f_{12} - 2f_{44}\right)}{c_{44}}\right]\frac{\partial P_3}{\partial x_1} + f_{44}\varepsilon_{13}^0 = 0\\
&a_1^S P_2 + \left(g_{44} - \frac{2f_{44}^2}{c_{44}}\right)\frac{\partial P_2}{\partial x_3} + \left[g_{44} + \frac{f_{44}\left(-f_{12} - 2f_{44}\right)}{c_{44}}\right]\frac{\partial P_3}{\partial x_2} + f_{44}\varepsilon_{23}^0 = 0\\
&a_1^S P_3 + \left[g_{12} - \frac{f_{11}\left(f_{12} + \frac{1}{2}f_{44}\right)}{2c_{44}}\right]\left(\frac{\partial P_1}{\partial x_1} + \frac{\partial P_2}{\partial x_2}\right) + \left(g_{11} - \frac{f_{11}^2}{2c_{11}}\right)\frac{\partial P_3}{\partial x_3}\\
&\quad + \frac{1}{2}\left(f_{12} - \frac{c_{12}}{c_{11}}f_{11}\right)\left(\varepsilon_{11} + \varepsilon_{22}\right) + \frac{1}{2}f_{11}\left(\frac{c_{12}}{c_{11}}\varepsilon_{11}^0 + \frac{c_{12}}{c_{11}}\varepsilon_{22}^0 + \varepsilon_{33}^0\right) = 0.
\end{aligned} \qquad (x_3 = h_f), \quad \text{(A5.2)}$$

By neglecting the nonlinear terms and in-plane polarization gradient terms, which are relatively small for the case of positive extrapolation length adopted in the present study, we can rewrite the boundary conditions as:

$$\begin{aligned}
&a_1^S P_1 - \left(g_{44} - \frac{2f_{44}^2}{c_{44}}\right)\frac{\partial P_1}{\partial x_3} = 0\\
&a_1^S P_2 - \left(g_{44} - \frac{2f_{44}^2}{c_{44}}\right)\frac{\partial P_2}{\partial x_3} = 0 \quad (x_3 = 0),\\
&a_1^S P_3 - \left(g_{11} - \frac{f_{11}^2}{2c_{11}}\right)\frac{\partial P_3}{\partial x_3} = 0;
\end{aligned} \qquad \text{(A6.1)}$$

$$\begin{aligned}
&a_1^S P_1 + \left(g_{44} - \frac{2f_{44}^2}{c_{44}}\right)\frac{\partial P_1}{\partial x_3} = 0,\\
&a_1^S P_2 + \left(g_{44} - \frac{2f_{44}^2}{c_{44}}\right)\frac{\partial P_2}{\partial x_3} = 0 \quad (x_3 = h_f),\\
&a_1^S P_3 + \left(g_{11} - \frac{f_{11}^2}{2c_{11}}\right)\frac{\partial P_3}{\partial x_3} = 0.
\end{aligned} \qquad \text{(A6.2)}$$

References

1. Mashkevich, V., Tolpygo, K.: Electrical, optical and elastic properties of diamond type crystals. I. Sov. Phys. JETP **5**, 435–439 (1957)
2. Kogan, S.M.: Piezoelectric effect under an inhomogeneous strain and acoustic scattering of carriers in crystals. Fiz. Tverd. Tela **5**, 2829–2831 (1963)
3. Ma, W.H., Cross, L.E.: Observation of the flexoelectric effect in relaxor Pb(Mg1/3Nb2/3)O-3 ceramics. Appl. Phys. Lett. **78**, 2920–2921 (2001)
4. Ma, W.H., Cross, L.E.: Flexoelectric polarization of barium strontium titanate in the paraelectric state. Appl. Phys. Lett. **81**, 3440–3442 (2002)

5. Ma, W.H., Cross, L.E.: Strain-gradient-induced electric polarization in lead zirconate titanate ceramics. Appl. Phys. Lett. **82**, 3293–3295 (2003)
6. Ma, W.H., Cross, L.E.: Flexoelectric effect in ceramic lead zirconate titanate. Appl. Phys. Lett. **86**, 072905 (2005)
7. Zubko, P., Catalan, G., Buckley, A., Welche, P.R.L., Scott, J.F.: Strain-gradient-induced polarization in SrTiO3 single crystals. Phys. Rev. Lett. **99**, 167601 (2007)
8. Catalan, G., Sinnamon, L.J., Gregg, J.M.: The effect of flexoelectricity on the dielectric properties of inhomogeneously strained ferroelectric thin films. J. Phys-Condens. Mat. **16**, 2253–2264 (2004)
9. Catalan, G., Noheda, B., McAneney, J., Sinnamon, L.J., Gregg, J.M.: Strain gradients in epitaxial ferroelectrics. Phys. Rev. B. **72**, 020102 (2005)
10. Maranganti, R., Sharma, N.D., Sharma, P.: Electromechanical coupling in nonpiezoelectric materials due to nanoscale nonlocal size effects: Green's function solutions and embedded inclusions. Phys. Rev. B. **74**, 014110 (2006)
11. Sharma, N.D., Maranganti, R., Sharma, P.: On the possibility of piezoelectric nanocomposites without using piezoelectric materials. J. Mech. Phys. Solids **55**, 2328–2350 (2007)
12. Eliseev, E.A., Morozovska, A.N., Glinchuk, M.D., Blinc, R.: Spontaneous flexoelectric/flexomagnetic effect in nanoferroics. Phys. Rev. B. **79**, 165433 (2009)
13. Chen, H.T., Soh, A.K.: Influence of flexoelectric effects on multiferroic nanocomposite thin bilayer films. J. Appl. Phys. **112**, 074104 (2012)
14. Shen, S.P., Hu, S.L.: A theory of flexoelectricity with surface effect for elastic dielectrics. J. Mech. Phys. Solids **58**, 665–677 (2010)
15. Majdoub, M.S., Sharma, P., Cagin, T.: Enhanced size-dependent piezoelectricity and elasticity in nanostructures due to the flexoelectric effect. Phys. Rev. B. **77**, 125424 (2008)
16. Lee, D., Yoon, A., Jang, S.Y., Yoon, J.G., Chung, J.S., Kim, M., Scott, J.F., Noh, T.W.: Giant flexoelectric effect in ferroelectric epitaxial thin films. Phys. Rev. Lett. **107**, 057602 (2011)
17. Sharma, N.D., Landis, C.M., Sharma, P.: Piezoelectric thin-film superlattices without using piezoelectric materials. J. Appl. Phys. **108**, 024302 (2010)
18. Lu, H., Bark, C.W., de los Ojos, D.E., Alcala, J., Eom, C.B., Catalan, G., Gruverman, A.: Mechanical writing of ferroelectric polarization. Science **336**, 59–61 (2012)
19. Lu, H., Kim, D.J., Bark, C.W., Ryu, S., Eom, C.B., Tsymbal, E.Y., Gruverman, A.: Mechanically-induced resistive switching in ferroelectric tunnel junctions. Nano. Lett. **12**, 6289–6292 (2012)
20. Zhou, H., Hong, J.W., Zhang, Y.H., Li, F.X., Pei, Y.M., Fang, D.N.: External uniform electric field removing the flexoelectric effect in epitaxial ferroelectric thin films. Epl-Europhys. Lett. **99**, 47003 (2012)
21. Catalan, G., Lubk, A., Vlooswijk, A.H.G., Snoeck, E., Magen, C., Janssens, A., Rispens, G., Rijnders, G., Blank, D.H.A., Noheda, B.: Flexoelectric rotation of polarization in ferroelectric thin films. Nat. Mater. **10**, 963–967 (2011)
22. Hu, H.L., Chen, L.Q.: Three-dimensional computer simulation of ferroelectric domain formation. J. Am. Ceram. Soc. **81**, 492–500 (1998)
23. Wang, Y.U., Jin, Y.M.M., Khachaturyan, A.G.: Phase field microelasticity modeling of dislocation dynamics near free surface and in heteroepitaxial thin films. Acta. Mater. **51**, 4209–4223 (2003)
24. Chen, H.T., Hong, L., Soh, A.K.: Effects of film thickness and mismatch strains on magnetoelectric coupling in vertical heteroepitaxial nanocomposite thin films. J. Appl. Phys. **109**, 094102 (2011)
25. Yurkov, A.S.: Elastic boundary conditions in the presence of the flexoelectric effect. Jetp Lett+ **94**, 455–458 (2011)
26. Morozovska, A.N., Eliseev, E.A., Kalinin, S.V., Chen, L.Q., Gopalan, V.: Surface polar states and pyroelectricity in ferroelastics induced by flexo-roto field. Appl. Phys. Lett. **100**, 142902 (2012)
27. Karthik, J., Mangalam, R.V.K., Agar, J.C., Martin, L.W.: Large built-in electric fields due to flexoelectricity in compositionally graded ferroelectric thin films. Phys. Rev. B. **87**, 024111 (2013)
28. Nambu, S., Sagala, D.A.: Domain formation and elastic long-range interaction in ferroelectric perovskites. Phys. Rev. B. **50**, 5838 (1994)
29. Pertsev, N.A., Zembilgotov, A.G., Tagantsev, A.K.: Effect of mechanical boundary conditions on phase diagrams of epitaxial ferroelectric thin films. Phys. Rev. Lett. **80**, 1988–1991 (1998)
30. Maranganti, R., Sharma, P.: Atomistic determination of flexoelectric properties of crystalline dielectrics. Phys. Rev. B. **80**, 054109 (2009)
31. Lo, V.C.: Simulation of thickness effect in thin ferroelectric films using Landau–Khalatnikov theory. J. Appl. Phys. **94**, 3353–3359 (2003)
32. Hong, L., Soh, A.K., Song, Y.C., Lim, L.C.: Interface and surface effects on ferroelectric nano-thin films. Acta. Mater. **56**, 2966–2974 (2008)
33. Liu, G., Nan, C.W.: Thickness dependence of polarization in ferroelectric perovskite thin films. J. Phys. D.: Appl. Phys. **38**, 584–589 (2005)
34. Sinnamon, L.J., Bowman, R.M., Gregg, J.M.: Thickness-induced stabilization of ferroelectricity in SrRuO3/Ba0.5Sr0.5TiO3/Au thin film capacitors. Appl. Phys. Lett. **81**, 889–891 (2002)
35. Li, Y.L., Hu, S.Y., Liu, Z.K., Chen, L.Q.: Effect of substrate constraint on the stability and evolution of ferroelectric domain structures in thin films. Acta. Mater. **50**, 395–411 (2002)